

Volume dependence of the Pauli susceptibility and the amplitude of the wave functions for potassium metal

Toshimoto Kushida, J. C. Murphy, and M. Hanabusa*

Research Staff, Ford Motor Company, Dearborn, Michigan 48121

(Received 19 June 1979)

The pressure dependence of the Knight shift K_N and the Pauli susceptibility χ_P in potassium metal were measured as a function of volume. χ_P was measured at 4.2°K and the maximum pressure was 5.5 kbar. The amplitude of the conduction-electron wave functions $\langle |\psi(0)|^2 \rangle$ derived using a standard Knight-shift equation is *not* a monotonic function of the volume. A recent calculation adequately describes the experimental results. Recent χ_P calculations for jellium agree with each other in spite of their apparently different formalisms. Shastry indicated, however, that the mutual agreement, which was once believed to be evidence for the validity of these theories, is *not* a proof, since they are equivalent to the same generalized random-phase approximation (RPA) theory (G-RPA). The present result for K in conjunction with the previous measurements for Li and Na provides experimental proof that (i) G-RPA is correct for $r_s \lesssim 4$ and that (ii) for $r_s > 4$, the jellium χ_P is somewhat smaller than the G-RPA result.

I. INTRODUCTION

The pressure-dependence measurement of the Pauli susceptibility in Li and Na (referred to hereafter as I)¹ revealed a susceptibility enhancement due to an exchange-correlation (XC) effect as a function of interelectronic distance. The calculation of the XC enhancement of the susceptibility χ_P/χ_F for a jellium model has been one of the favorite subjects of theoreticians for the past 50 years.² Here χ_P and χ_F are the Pauli susceptibility of the interacting and the noninteracting electron gas, respectively.

Although the alkali metals, particularly Na and K, are the closest replicas of the jellium model, Vosko and his collaborators³⁻⁷ found that a crystalline-effect correction is important for a critical evaluation of these jellium theories using experimental results. A new theory developed by these authors [referred to as a Vosko-Perdew (VP) theory] enables one to calculate the Pauli susceptibility of an inhomogeneous electron gas. The inhomogeneity of the charge density and that of the magnetic-moment distribution are caused by the electronic structures of real metals. Good agreement between the experimental results for Li and Na and the *ab initio* calculations based on the VP theory strongly indicates that a *consensus curve* in Fig. 6 of I⁸ is basically correct up to $r_s \approx 4$ and that the VP theory can adequately handle a large crystalline effect in Li. Here r_s is the usual electron-density parameter.

It was originally thought that a close agreement among many theories, seemingly derived from different models, was a proof of the correctness of the consensus curve.⁹ Shastry^{10,11} has, however, pointed out that these theories are essentially based on the same RPA (random-phase

approximation) model and that the mutual agreement does not guarantee the validity of the consensus curve. An experimental proof is still important. Besides, more recent theoretical attempts to go beyond the RPA suggest^{12,13} that the χ_P/χ_F curve may flatten off at large r_s . A comparison between the VP calculations and the observed χ_P/χ_F values for K, Rb, and Cs seems to indicate the same tendency.⁶

The volume-dependence measurement of χ_P for K metal is informative. The derived slope $d(\chi_P/\chi_F)/dr_s$ in conjunction with the available value of χ_P/χ_F for K ($r_s = 4.86$) would yield an insight into the XC effect in the low-density-metal region ($r_s > 4$). The experimental difficulties are, however, much more severe than those for Li and Na.

The Knight-shift measurement yields direct information¹⁴ on the amplitude of the conduction-electron wave functions *provided* χ_P is known. In simple metals the Knight shift K_N is

$$K_N = \frac{8\pi}{3} \chi_P \Omega P_F. \quad (1)$$

Here χ_P is the Pauli susceptibility in cgs volume units, Ω is the atomic volume, and $P_F [= \langle |\psi_F(0)|^2 \rangle]$ is the amplitude of the conduction-electron wave functions at the position of the nucleus averaged over the Fermi surface. The volume dependence of K_N for all the alkali metals except K was measured in 1958.¹⁵ Here we report the pressure measurement of K_N for K metal. The measured volume dependence of χ_P and K_N gives the volume dependence of P_F by using Eq. (1). The experimentally derived $P_F(V)$ is markedly different from a previous theoretical prediction¹⁶ but in reasonable agreement with a recent calculation.¹⁷

II. EXPERIMENTAL PROCEDURE AND RESULTS

A. Pressure dependence of the Knight shift

High-purity K metal was purchased from MSA.¹⁸ The bulk metal was ultrasonically dispersed in a light mineral oil. The details of the experimental procedure have been described elsewhere.¹⁹ The magnetic field was stabilized during the pressure run by locking the field to the NMR line of Na metal dispersion. The Na NMR was detected with a frequency-stabilized rf spectrometer. The NMR line of K metal was recorded on a chart recorder. Since the NMR line is very narrow, the resonance frequency could be measured precisely without using a signal-averaging technique.¹⁹ The center frequency of the NMR line was measured as a function of hydrostatic

pressure at room temperature.

The results are shown in Fig. 1. The pressure dependence of the resonance frequency was converted into a volume dependence of the Knight shift using available data for the compressibility²⁰ and the Knight shift [$K_N = 0.261\%$ (Ref. 21)]. Figure 2 shows the results where the volume is normalized to the atmospheric value $V(0)$.

It is noted that K_N is *not* a monotonic function of volume in contrast to the earlier prediction.¹⁶ As the pressure is increased from the atmospheric value, K_N decreases first, reaches a minimum at approximately 800 kg/cm², and increases at higher pressure.

It is interesting to compare this result with the pressure dependence of other alkali metals Na, Rb, and Cs (Ref. 15):

$$\left(\frac{d \ln K_N}{dP}\right)_{\text{Na}} < \left(\frac{d \ln K_N}{dP}\right)_{\text{K, low pressure}} < 0 < \left(\frac{d \ln K_N}{dP}\right)_{\text{K, high pressure}} < \left(\frac{d \ln K_N}{dP}\right)_{\text{Rb}} < \left(\frac{d \ln K_N}{dP}\right)_{\text{Cs}}$$

The sign and the magnitude of the pressure dependence of K_N changes systematically as a function of atomic weight. The sign of $d \ln K_N/dP$ changes at K.

B. Pressure dependence of χ_P

The original intention was to measure the pressure dependence of χ_P in K with the Schumacher-

Slichter method as described in I. The principle of this method is to measure the area under the conduction-electron spin resonance (CESR) absorption curve A_e , which is proportional to χ_P ,²² as a function of pressure. The gain of the rf spectrometer system is calibrated by measuring the NMR absorption area A_n in the same sample by increasing the magnetic field. χ_P is obtained in terms of a well defined nuclear susceptibility χ_P^n as

$$\chi_P = \chi_P^n (\gamma_e/\gamma_n) (A_e/A_n). \quad (2)$$

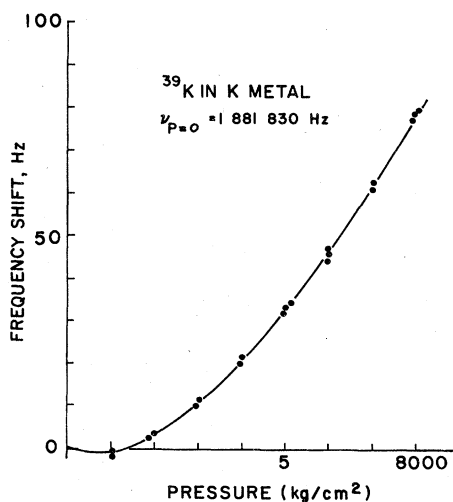


FIG. 1. Pressure dependence of the Knight shift in K metal. The increase of the resonance frequency is not monotonic with respect to the volume reduction. The data were taken at the room temperature.

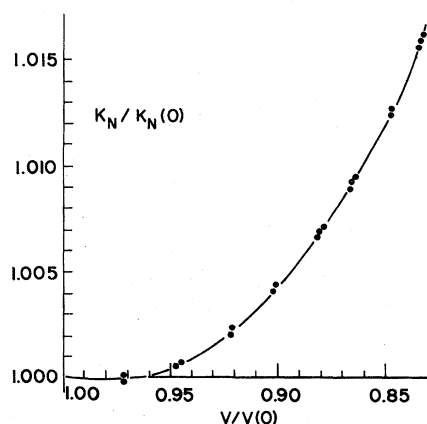


FIG. 2. Volume dependence of the Knight shift K_N in K metal. Both K_N and the volume V are normalized to their atmospheric values, respectively.

Here γ_e and γ_n are the electronic and the nuclear gyromagnetic ratios, respectively. The essential experimental setup is shown in Fig. 1 of I.

The measurement for K was much more difficult than that for Li and Na for various reasons, and some modification was necessary. The CESR linewidth of K at room temperature is much larger because of a larger spin-orbit coupling. Since the Schumacher-Slichter method requires one to measure the CESR at a low magnetic field (≤ 10 G), the CESR linewidth must be of the same order of magnitude as, or preferably smaller than, this field value. The measurement of the K CESR had to be done at liquid-helium temperature in order to reduce the linewidth. The spurious EPR signals due to paramagnetic impurities increase their intensity as $1/T$ as the temperature T is decreased, whereas the CESR intensity is virtually temperature independent. The interference of the impurity EPR signals becomes more serious at low temperature. Some of the impurity EPR signals are pressure dependent. It is important to eliminate paramagnetic impurities from the sample as well as from the inside of the sample container. The cleanliness of the rf coil is also crucial.

Since the rf skin depth of the high-purity K sample decreases at low temperature, the particle size of the dispersed sample must be smaller for the low-temperature measurements. If the particle size is too small, however, the rate of the surface scattering of the electrons increases; thereby the linewidth tends to increase. The chance of sample contamination increases also.

Since the linewidth of the ^{39}K NMR line is narrow (~ 3.5 G) due to a weak dipole-dipole interaction, it was very difficult to avoid saturation of the NMR line at the low temperature. The oscillation level of the present Pound-Knight-Watkins-type spectrometer could not be reduced sufficiently. Even if one uses a bridge-type spectrometer where the rf intensity can be reduced to any level, it is doubtful that such a low rf level provides a sufficient signal intensity for the CESR line.

We had to abandon the original scheme of the Schumacher-Slichter method where the NMR signal in the same CESR sample was used as an intensity calibrator. We used instead the NMR signal of Al metal powder, which is less saturable, as the calibrator. Merely mixing a proper amount of Al powder with the K dispersion was not adequate. The Al and the K powder tended to segregate during the pressure change. We made a honeycomb-shaped sample container with Al-powder-impregnated epoxy²³ (Fig. 3). The longitudinal holes in the honeycomb were filled

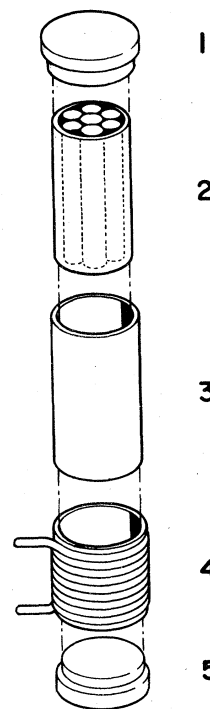


FIG. 3. Sample holder assembly for the pressure dependence measurement of the K-metal Pauli susceptibility. 1: an epoxy cap; 2: a honeycomb structure made of Al-powder-impregnated epoxy. The holes of the honeycomb were filled with K-metal dispersion. The Al NMR signal was used for the sensitivity calibration of an rf spectrometer. 3: a Mylar sleeve; 4: an rf coil; 5: an epoxy bottom.

with the K dispersion. We did not attempt to measure the absolute value of χ_P . Only the change in χ_P , with respect to pressure was measured.²⁴

Although the CESR of the Al powder might have increased the observed value of χ_P somewhat, the contribution to the observed pressure change is negligible within the present experimental error. The compressibility of Al is only $\frac{1}{20}$ of that of K. The CESR linewidth of Al is much larger; we scanned only a small portion of the Al line. The purity of the Al powder was not high.

The high-purity K metal was ultrasonically dispersed in light mineral oil. The dispersion process was critical for the CESR sample preparation; many dispersed samples had to be discarded. The particle size was either too large or too small. Satisfactory samples consist of relatively uniform-size particles. The diameter of the particles was approximately $2 \mu\text{m}$.

High pressure at 4.2°K was generated by cooling a compressed liquid in a high-pressure bomb.²⁵ The pressure transmitting fluid was a 50-50 mixture of petroleum ether and transformer

oil (Shell Dial-A oil AX). The fluid in the pressure bomb was compressed up to approximately 8000 kg/cm² at about 0°C. The bomb was slowly cooled to 4.2°K. Because of the difference in thermal contraction between the bomb material (Be-Cu) and the fluid, the pressure in the bomb decreased by ~40% as the temperature was reduced. The actual pressure at the low temperature was measured by monitoring the superconducting transition temperature T_c of a small piece of Sn in the bomb. The transition could be easily observed by a sudden increase in the Q value of the rf coil. Thus no extra high-pressure feedthrough was required. After completing the susceptibility measurement, the liquid He in the Dewar was pumped slowly. A small ac magnetic field was applied from the outside of the bomb during the pump down. Thus the T_c value was modulated. The surface resistance of the Sn piece and thereby the Q value of the rf coil was strongly modulated as the temperature went through T_c . The modulation of Q was phase detected as usual and monitored on a recorder. From the vapor pressure reading of He at the peak of the recorder deflection, T_c was obtained accurately. The effect of the dc component of the modulation field was checked and corrected when it was necessary.

The pressure in the bomb P was derived by using an empirical equation obtained by Jennings and Swenson²⁶:

$$T_c = 3.732 - 4.95 \times 10^{-5}P + 3.9 \times 10^{-10}P^2, \quad (3)$$

where T_c is in °K and P is in atm. Since the thermal contraction between 4.2°K and T_c is negligible, the pressure value at T_c is safely equated to the pressure at 4.2°K.

Although the ²⁷Al NMR line is less saturable than the ³⁹K line, there was some saturation at 4.2°K. The apparent intensity of the NMR decreases due to saturation as $(1 + aH_1^2)^{-1}$; if the condition $H_1^2 \ll 1$ is not satisfied,²⁷ the observed value of A_o/A_n changes with H_1 as $1 + aH_1^2$, where a is a constant and H_1 is the amplitude of the rf magnetic field in the sample. The true χ_p value can be extrapolated²⁸ by plotting the observed A_o/A_n against the square of the rf voltage across the rf coil v^2 , which is proportional to H_1^2 .

When the CESR line was observed, the magnetic field was swept linearly through zero field back and forth (Fig. 1 in I). The amplitude of the triangular sweep was between ± 60 and ± 180 G. The observed CESR line width was 5.1 G full width at half maximum (FWHM) at atmospheric pressure (Fig. 4) and increased to 11.3 G at 4900 kg/cm² (Fig. 5). The A_o/A_n values were measured as a function of the sweep amplitude both at zero and at the high pressure. The pressure shift in

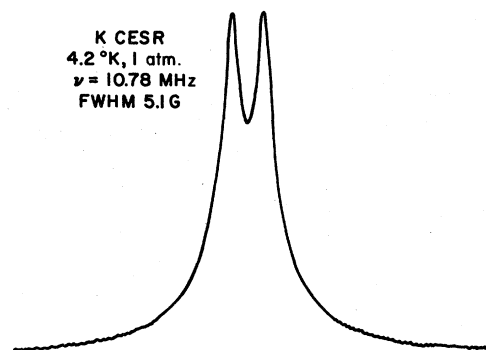


FIG. 4. K CESR line at 1 atm and 4.2°K. The spectrometer frequency was 10.78 MHz. The observed curve is the superposition of two Lorentzian resonance curves whose full width at half maximum (FWHM) is 5.1 G.

A_o/A_n was extrapolated to the value for an infinite sweep amplitude. The extrapolation procedure is described in the Appendix. The extrapolation was necessary, since the linewidth increased considerably at the high pressure. It was found that this procedure was a convenient way to check the degree of interference caused by the possible impurity EPR lines. The spectrometer frequency was 10.78 MHz.

The data-taking procedures are summarized as follows. The pressure bomb was cooled to 4.2°K in the morning. The A_n value was accumulated 64 times, and the results were printed out. Then A_o was measured in the same way. These sequences were repeated 5 times. The same set of measurements was performed at five different modulation fields. The rf level was changed in five steps to get the unsaturated values for the NMR intensity. It took a whole day to complete these procedures. The next morning the bomb

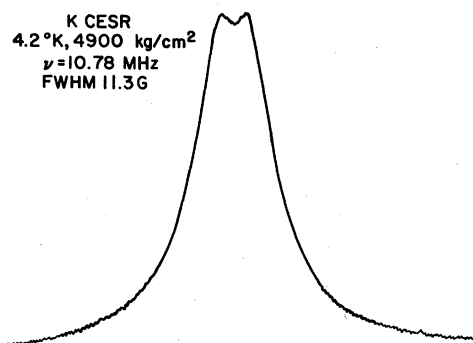


FIG. 5. K CESR line at high pressure. The pressure and the temperature were 4900 kg/cm² and 4.2°K, respectively. The linewidth increased considerably with the pressure probably due to the strain in the sample induced by the freezing under high pressure.

was warmed up to near 0° by sending warm He gas followed by dry air into the Dewar. The bomb was then pressurized and cooled down to 4.2°K . The same measuring procedures described above were repeated. After the CESR and the NMR measurements at the particular pressure were completed, the He in the Dewar was pumped slowly, and the T_c value of the Sn piece in the bomb was observed. The pressure was released after warming up the bomb, and the bomb was cooled again. The zero-pressure measurements were carried out again on the third day. The data at a different pressure were taken the next day. It took several days to complete a set of the pressure measurements.

The observed pressure dependence of the susceptibility is the change in the atomic susceptibility χ_P^A . The number of atoms does not change with volume compression. The observed relative change in the atomic susceptibility $\chi_P^A(V)/\chi_P^A(0)$ can be converted to the change in volume susceptibility by using the relation

$$\chi_P(V)/\chi_P(0) = [\chi_P^A(V)/\chi_P^A(0)]/[V/V(0)].$$

The volume susceptibility $\chi_P(V)$ is used in most of the theories. The results are shown in Fig. 6. The data points represent the assembly of data

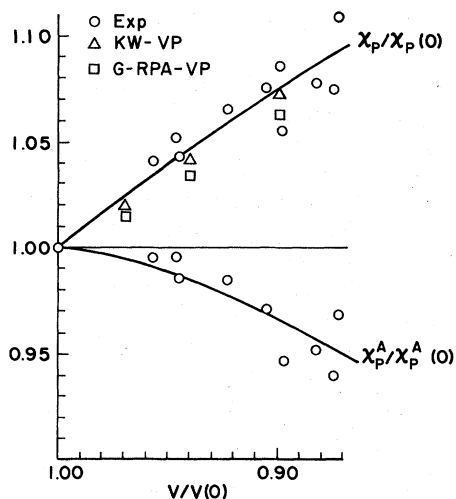


FIG. 6. Volume dependence of the Pauli susceptibility in K. \circ are the experimental values. χ_P^A and χ_P are atomic and volume susceptibility, respectively. The susceptibility and the volume are normalized to their atmospheric values, respectively. The measured susceptibility change is the change in χ_P^A . The χ_P change was derived using the relation $\chi_P(V)/\chi_P(0) = [\chi_P^A(V)/\chi_P^A(0)]/[V/V(0)]$. Δ : theoretical values, the jellium susceptibility by KW (Fig. 8) with the crystal-line effect correction (VP), Ref. 42. \square : theoretical values, the same calculation but based on the G-RPA jellium susceptibility, Ref. 42.

obtained with several different samples. The scattering of the data points is relatively large, compared with the results for Li and Na (Fig. 4 in I) because of the experimental difficulties described above. The strain broadening of the CESR line may be responsible for the increase in scattering at the higher pressure points.

The assessment of error is difficult. The possible effect of the pressure-sensitive impurity EPR line is hardest to estimate. The previous experience with the Na measurement (I and Ref. 79 in I) indicates that this effect is strongly dependent on the samples. In the present experiment the difference in the data for the different samples was not greater than the data scattering for each individual sample. The impurity effect may therefore be within the scattering of the data shown in the figure.

In spite of the data scattering, the difference between the K and the Na results is quite evident. $|d \ln \chi_P/d \ln V|$ for K is approximately twice as large as that of Na. The deviation from the free-electron value, $d \ln \chi_F/d \ln V = -\frac{1}{3}$, is clear. This is another example of the fact that one has to take a realistic value of $d \ln \chi_P/d \ln V$ rather than its free-electron value in order to derive $d \ln P_F/d \ln V$ from the experimental value of $d \ln K_N/d \ln V$ using Eq. (1). This has been suggested by many experimentalists²⁹ but has been ignored by some theoreticians who want to compare their calculated $P_F(V)$ values with the experimental results.

C. The volume dependence of P_F

The volume dependence of P_F is derived from

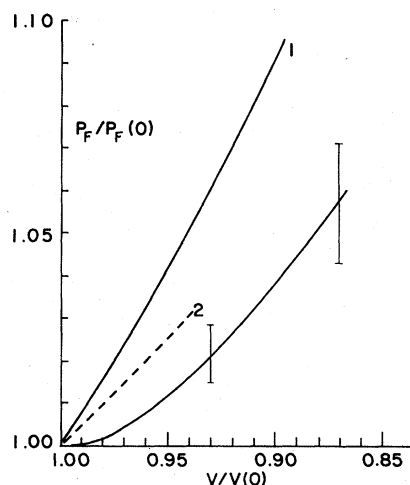


FIG. 7. Volume dependence of P_F . P_F , P_F , and V are normalized to their atmospheric values, respectively. 1: Asano and Yamashita, Ref. 16. 2: Moore and Vosko, Ref. 30. The recent calculation by Vosko *et al.*, Ref. 17, agrees with the experimental results.

$K_N/K_N(0)$ (Fig. 2) and $\chi_P/\chi_P(0)$ (Fig. 6) by using Eq. (1). The results are shown in Fig. 7. Again the error flags are quite large due to the scattering in the $\chi_P/\chi_P(0)$ data. It is still useful to assess the validity of the theoretical calculations.

III. COMPARISON WITH THEORIES

The theoretical predictions for $P_F(V)/P_F(0)$ are also shown in Fig. 7. Although the Asano and Yamashita calculation¹⁶ for Na is in close agreement with the experimental results (Fig. 5 in I), their prediction for K is more than twice as large as the experimental values. The Moore and Vosko estimate³⁰ is also shown in the figure.

The slope change in $K_N(V)$ near $V/V(0) \sim 0.97$ (Fig. 2) is not very clear in the experimental results in Fig. 7 due to the large error flags. It is, however, most likely that $\chi_P(V)$ is nearly a straight line. $P_F(V)$ may preserve the unique feature of $K_N(V)$ shown in Fig. 2. $P_F(V)$ is probably nearly flat at the small compression range, as is suggested in Fig. 7.

The recent calculations by Vosko *et al.*¹⁷ essentially reproduced the observed features of $P_F(V)$ and $K_N(V)$. They showed that the slope of these quantities changes markedly at the low compression range.

As stated earlier, the XC enhancement factor of the susceptibility of the homogeneous electron gas χ_P/χ_F has not been settled for large r_s ($r_s > 4$). In Fig. 8 the recent developments for χ_P/χ_F calculations, a few relevant previous curves (shown in I), and the correction of the figure in I (Ref. 2) are listed. The original Brueckner and Sawada's calculation³¹ which contained a numerical error¹¹ is shown as BS, which was misrepresented in I, Fig. 6. BS (corrected) is the corrected BS calculations.¹¹ This is exact at high density. Shastry^{10,11} showed that the calculations of DG (Dupree and Geldart³²), HO (Hamann and Overhauser³³), and VH (von Barth and Hedin³⁴) are essentially the same generalized RPA calculation (G-RPA) rediscovered using different methods. Shastry also indicated that Rice's calculation,³⁵ after his recalculation which corrected some typographical error, agrees with these results. One of the original results by Rice is shown as R-H. The calculations of VS (Vashishta and Singwi³⁶), PTV (Pizzimenti, Tosi, and Villari³⁷), and HL (Hedin and Lundqvist³⁸) also fit the G-RPA result.

The calculation of KW (Keiser and Wu³⁹) agrees with G-RPA for $r_s \leq 4$ (the difference is <10%) but tends to saturate at lower density. The calculation of KYW (Kawazoe, Yasuhara, and Watabe¹²) is a recent attempt within the framework of the gen-

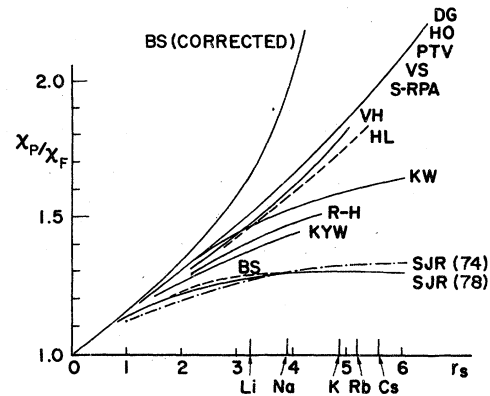


FIG. 8. Theoretical predictions for the many-body susceptibility enhancement χ_P/χ_F as a function of the Wigner-Seitz radius r_s . For a more extensive list, see Fig. 6 in Ref. 1. DG, Dupree and Geldart, Ref. 32; HO, Hamann and Overhauser, Ref. 33; PTV, Pizzimenti, Tosi, and Villari, Ref. 37; VS, Vashishta and Singwi, Ref. 36; S-RPA, RPA by Shastry, Ref. 11; VH, von Barth and Hedin, Ref. 34; HL, Hedin and Lundqvist, Ref. 38; KW, Keiser and Wu, Ref. 39; R-H, Rice, based on the Hubbard model, Ref. 35; KYW, Kawazoe, Yasuhara, and Watabe, Ref. 12; BS, Brueckner and Sawada, Ref. 31, which was misrepresented in Ref. 1 and in Ref. 104 of I; BS (corrected), Brueckner and Sawada as corrected by Shastry, Ref. 11; SJR (74) Shastry, Jha, and Rajagopal, Ref. 40; SJR (78), Shastry, Jha, and Rajagopal, Ref. 13.

eralized RPA. Their result at $r_s \sim 4$ is, however, considerably lower than the previous G-RPA. The SJR (74)⁴⁰ and SJR (78)¹³ (Shastry, Jha, and Rajagopal) calculations indicated that the susceptibility enhancement at the low metallic density range ($r_s \sim 6$) is much smaller than G-RPA. The SJR (78) calculation intended to go beyond the generalized RPA method.

All of these results are calculated for the idealized jellium model. Vosko and his collaborators³⁻⁷ showed that even for Na and K the correction due to the crystalline effect is important. The electron charge and the magnetic-moment distribution in real metals are not homogeneous. They indicated that this correction is particularly important when the volume dependence of the susceptibility enhancement is calculated. For example, the experimental value of $d(\chi_P/\chi_F)/dr_s$ for Na is almost zero (Table II in I).⁴¹ The slope of G-RPA at $r_s \sim 4$ is definitely positive (Fig. 8). Yet Vosko *et al.* showed that the calculated slope agrees perfectly with the experimental value when they take G-RPA as the homogeneous susceptibility enhancement and correct the crystalline effect using their newly developed method (VP).^{4,42} The experimental value of χ_P/χ_F for Na (Ref. 43) is, however, in reasonable agreement with the G-RPA

value without the VP correction. For Li, the VP correction is important both for χ_P/χ_F and $d(\chi_P/\chi_F)/dr_s$ (Table II in I); Li is far from being a jellium.

It is quite clear that G-RPA is correct^{1,6,11} for $r_s \lesssim 4$. The deviation from G-RPA may be significant for $r_s > 4$, however, as suggested by the recent calculations of KYW and SJR (78). The MacDonald and Vosko results⁶ also suggest that the jellium χ_P/χ_F tends to saturate for the low-density range. They showed that the VP calculation using the KW result gives better agreement with the observed χ_P for K, Rb, and Cs than the same calculation with the VH value.

Wilk *et al.*⁴² calculated the volume dependence of χ_P/χ_F for K with the VP theory using two jellium χ_P/χ_F values, G-RPA and KW. The results, G-RPA-VP and KW-VP, are shown in Fig. 6. KW-VP seems to be in better agreement with the experimental results.

It can be concluded that the previous (I) and the present experimental results indicate that the susceptibility enhancement for jellium is described correctly by G-RPA for $r_s \lesssim 4$ and that it is close to KW for $r_s > 4$. It is highly desirable to get a more accurate experimental answer for $r_s > 4$. The present method is, however, not suitable for the study of the lower-density alkali metals Rb and Cs. A large spin-orbit coupling in these metals makes the CESR linewidth excessively large for this method. Other methods, the spin wave²⁴ and the de Haas-van Alphen (dHvA) experiment,²⁴ are more appropriate to derive χ_P values for these metals.

Pinkel and Schultz⁴⁴ recently pointed out that there is some discrepancy between the experimental value of χ_P/χ_F for Rb derived from their spin-wave measurement and the VP calculations⁶; $(\chi_P/\chi_F)_{\text{exp}} = 1.56 \pm 0.1$ and the VP results, 1.73 to 1.93. The χ_P value derived from the dHvA measurement²⁴ 1.724 ± 0.010 is in agreement with the VP calculation, however. Another way to increase the low-density jellium information is to increase the accuracy of the volume-dependence measurement of χ_P for K. This method may have some advantage over the measurement of χ_P for Rb and Cs. K is a better jellium than Rb and Cs. The magnitude of the spin-orbit coupling and the nonsphericity of the Fermi surface, which are not taken into account in a standard Landau Fermi-liquid theory on which the analysis of the spin-wave experiment is based, are less important in K than in Rb and Cs. The relativistic effect, which may be important for the calculations of lighter metals,⁶ is negligible for K. It might be helpful to use higher pressure. The excessive broadening of the CESR line at the high pressure might be re-

duced by using an improved strain reducing technique.⁴⁵

IV. CONCLUSION

The pressure dependence of the Knight shift and the Pauli susceptibility in K metal yielded the volume dependence of the wave functions for the conduction electrons. The result is different from the previous theoretical predictions. It is in agreement with the new VP calculation. The observed volume dependence of the susceptibility indicates that the susceptibility enhancement of the low-density electron liquid ($r_s > 4$) is close to the Keiser and Wu result.

ACKNOWLEDGMENTS

We are indebted to Professor S. H. Vosko for discussion relating to the current experimental results and for private communication of his calculations prior to publication. We would like to express our gratitude to Professor B. Sriram Shastry for his private communication.

APPENDIX

The CESR absorption line area was measured with an electronic integrator (a voltage-to-frequency converter and an up-down counter) as described in I. The dc output level of a signal amplifier (0' in Fig. 9) was not necessarily equal to the real base line of the signal (0 in Fig. 9). The real base line was not seen clearly because of (i) the noise in the signal and (ii) the long tails of the Lorentzian line shape. Besides, the electronic base line might drift slowly. In order to circumvent this difficulty the following method was used. The integrator was operated in an up mode during the periods II and III and in a down mode during I and IV (Fig. 9). This procedure cancels the area between the base line of the

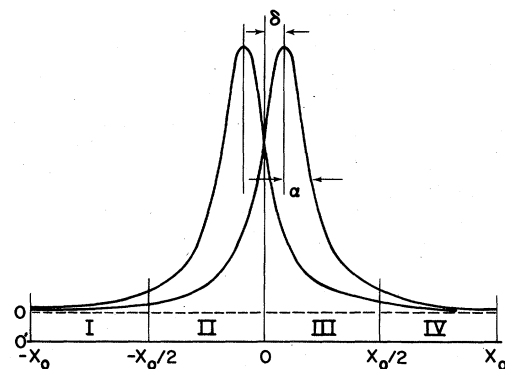


FIG. 9. Two identical Lorentzian profiles separated by 2δ . α is the half width at half maximum (HWHM).

resonance curve (0) and the electronic base line (0'). It is also noted that the effect of the base line slope, as long as it is linear, is also eliminated. If the modulation amplitude of the magnetic field is not sufficiently large, however, some of the tail area of the signal is also canceled. In fact the susceptibility value measured using this method for Li and Na are somewhat (5% to 10%) smaller than the recent measurement by Whiting *et al.*^{22,43} They estimated the far tail contribution to the total CESR area with a line-shape fitting. This correction was not important for the *pressure dependence* results of χ_p in Li and Na as discussed in I.

This is not the case in K. The maximum field sweep amplitude available, ± 180 G ($x_0 = 180$ G in Fig. 9), was not sufficient. The contribution to the pressure dependence from the tails beyond $\pm \frac{1}{2}x_0$ was not negligible.

Assuming the observed curve is a superposition of two identical Lorentzian curves displaced by 2δ (essentially the same assumption made by Whiting *et al.*²²), we can calculate the observed area $A(x_0)$ as

$$A(x_0) = - \int_{-x_0}^{-x_0/2} f(x) dx + \int_{-x_0/2}^{+x_0/2} f(x) dx - \int_{x_0/2}^{x_0} f(x) dx, \quad (\text{A1})$$

$$f(x) = \alpha \{ [\alpha^2 + (x + \delta)^2] + [\alpha^2 + (x - \delta)^2] \}.$$

Here δ is the resonance field and α is a half-

width at half-maximum value. When $x_0 > \alpha$ and δ , the leading terms are

$$A(x_0) = 2\pi - \frac{12\alpha}{x_0} + \dots$$

When $x_0 \rightarrow \infty$, the true area $A(\infty)$ becomes 2π .

$$A(x_0) = A(\infty) \left(1 - \frac{6\alpha}{\pi x_0} + \dots \right). \quad (\text{A2})$$

$A(\infty)$ can be deduced as the intercept of the observed area $A(x_0)$ plotted against $1/x_0$.

It is noted that a deviation from the original assumption would result in a deviation from the asymptotic linear relation between $A(x_0)$ and $1/x_0$. For example, a hidden broad impurity line located at zero field would give a nonlinear relation, since the retention of the leading term in (A2) is not sufficient for this line ($\alpha \approx x_0$). Impurity EPR lines which have zero-field splitting might be located at the inside or the outside of the sweep range $\pm x_0$. The result may show up as a deviation from the assumed Lorentzian curves. Indeed the actual plots were nearly straight lines, but some deviation was noted at the higher modulation amplitudes, suggesting a hidden broad impurity line at the center. The differences between the plots of the atmospheric pressure measurement and the high-pressure measurement was almost a straight line. The intercept of this line indicates the pressure shift in $A(\infty)$. The data with a marked deviation from this behavior were discarded.

*Present address: Toyohashi Technical University, Toyohashi, Japan.

¹Toshimoto Kushida, J. C. Murphy, and M. Hanabusa, *Phys. Rev. B* **13**, 5136 (1976); **15**, 1231 (E) (referred to as I). An extensive list of the literature is included in I.

²See Fig. 6 in I. For the correction of this figure, see Fig. 8 in this paper and Ref. 11.

³S. H. Vosko, J. P. Perdew, and A. H. MacDonald, *Phys. Rev. Lett.* **35**, 1725 (1975).

⁴S. H. Vosko and J. P. Perdew, *Can. J. Phys.* **53**, 1385 (1975).

⁵A. H. MacDonald, J. P. Perdew, and S. H. Vosko, *Solid State Commun.* **18**, 85 (1976).

⁶A. H. MacDonald and S. H. Vosko, *J. Low Temp. Phys.* **25**, 27 (1976).

⁷S. H. Vosko, *Bull. Am. Phys. Soc.* **22**, 359 (1977).

⁸DG, HO, PTV, VS, BH, HL', and L-RPA in Fig. 6 of I.

⁹For literature, see I.

¹⁰B. Sriram Shastry, *Phys. Rev. Lett.* **38**, 449 (1977).

¹¹B. Sriram Shastry, *Phys. Rev. B* **17**, 385 (1978). The authors are grateful for pointing out a misrepresentation of the BS curve in Fig. 6 in I. A similar error

was found in Ref. 104 in I.

¹²Y. Kawazoe, H. Yasuhara, and M. Watabe, *J. Phys. C* **10**, 3293 (1977).

¹³B. Sriram Shastry, Sudhanshu S. Jha, and A. K. Rajagopal, *Phys. Rev. B* **18**, 2616 (1978).

¹⁴See I for detailed discussion.

¹⁵G. B. Benedek and T. Kushida, *J. Phys. Chem. Solids* **5**, 241 (1958).

¹⁶Seturo Asano and Jiro Yamashita, *J. Phys. Soc. Jpn.* **34**, 1223 (1973).

¹⁷S. H. Vosko (private communication); L. Wilk and S. H. Vosko, *Bull. Am. Phys. Soc.* **24**, 490 (1979).

¹⁸MSA Research Corporation, Gallery, PA 16024.

¹⁹Toshimoto Kushida and J. C. Murphy, *Phys. Rev. B* **3**, 1574 (1971).

²⁰S. N. Vaidya, I. C. Getting, and G. C. Kennedy, *J. Phys. Chem. Solids* **32**, 2545 (1971).

²¹ $K_F = 0.261 \pm 0.002\%$, 25 °C, [M. P. Klein and W. D. Knight, *J. Phys. Chem. Solids* **15**, 355 (1960)]. Other available data are $0.265 \pm 0.002\%$, 25 °C, [W. H. Jones, Jr., T. P. Graham, and R. G. Barnes, *Acta Metall.* **8**, 663 (1960)], $0.248 \pm 0.005\%$, 25 °C [F. J. Milford and W. B. Gager, *Phys. Rev.* **121**, 716 (1961)], and 0.251

- $\pm 0.005\%$ [W. B. Gager and F. J. Milford, *Bull. Am. Phys. Soc.* **5**, 176 (1960)].
- ²²B. R. Whiting, N. S. VanderVen, and R. T. Schumacher, *Phys. Rev. B* **18**, 5413 (1978).
- ²³Hardman extra fast setting epoxy (Hardman Inc., Denville, N. J.) was used, since it is EPR-signal free.
- ²⁴The absolute value of χ_p at atmospheric pressure has been measured using different methods [G. L. Dunifer, D. Pinkel, and S. Schultz, *Phys. Rev. B* **10**, 3159 (1974); B. Knecht, *J. Low Temp. Phys.* **21**, 619 (1975)].
- ²⁵E. S. Ikskevich, *Cryogenics* **4**, 365 (1964).
- ²⁶L. D. Jennings and C. A. Swenson, *Phys. Rev.* **112**, 31 (1958).
- ²⁷For instance, E. R. Andrew, *Nuclear Magnetic Resonance* (Cambridge University, London, 1958) p. 20.
- ²⁸J. E. Kettler, W. L. Shanholtzer, and W. E. Vehse, *J. Phys. Chem. Solids* **30**, 665 (1969).
- ²⁹G. A. Matzkanin and T. A. Scott, *Phys. Rev.* **151**, 360 (1966); F. Borsa and R. G. Barnes, *J. Phys. Chem. Solids* **27**, 567 (1966); Toshimoto Kushida and J. C. Murphy, *Phys. Rev.* **178**, 433 (1969).
- ³⁰R. A. Moore and S. H. Vosko, *Can. J. Phys.* **46**, 1425 (1968).
- ³¹K. A. Brueckner and K. Sawada, *Phys. Rev.* **112**, 328 (1958).
- ³²R. Dupree and D. J. W. Geldart, *Solid State Commun.* **9**, 145 (1971).
- ³³D. R. Hamann and A. W. Overhauser, *Phys. Rev.* **143**, 183 (1966).
- ³⁴U. von Barth and L. Hedin, *J. Phys. C* **5**, 1629 (1972).
- ³⁵T. M. Rice, *Ann. Phys. (N.Y.)* **31**, 100 (1965). The results are shown in Fig. 6 of I as R-H and R-NP.
- ³⁶P. Vashishta and K. S. Singwi, *Solid State Commun.* **13**, 901 (1973).
- ³⁷G. Pizzimenti, M. P. Tosi and A. Villari, *Nuovo Cimento* **2**, 81 (1971).
- ³⁸L. Hedin and S. Lundqvist, *J. Phys. (Paris)* **33**, Suppl. C3, 73 (1972).
- ³⁹G. Keiser and F. Y. Wu, *Phys. Rev. A* **6**, 2369 (1972).
- ⁴⁰B. Sriram Shastry, Sudhanshu S. Jha, and A. K. Rajagopal, *Phys. Rev. B* **9**, 2000 (1974).
- ⁴¹ $d(\chi_P/\chi_F)/d\tau_s = 0.04 \pm 0.03$. The volume dependence of χ_P (Fig. 4 in I) is almost the same as that of χ_F .
- ⁴²L. Wilk, A. H. MacDonald, and S. H. Vosko, (unpublished.) Figure 2 in this literature indicates that both G-RPA and KW give good agreements with the experiment for Na.
- ⁴³ $(\chi_P/\chi_F)_{\text{exp}} = 1.683 \pm 0.018$. The most recent measurement of χ_P for Na gives $\chi_P = (1.092 \pm 0.012) \times 10^{-6}$ cgs volume unit at 77 °K [B. R. Whiting, N. S. VanderVen, and R. T. Schumacher, *Ref. 22*; *Bull. Am. Phys. Soc.* **22**, 533 (1977)]. $(\chi_P/\chi_F)_{\text{exp}}$ is derived from this value for χ_P and the relation $\chi_F = 2.589 \tau_s^{-1} \times 10^{-6}$ with $\tau_s = 3.99$.
- ⁴⁴Daniel Pinkel and Sheldon Schultz, *Phys. Rev. B* **18**, 6639 (1978).
- ⁴⁵N. B. Brandt, S. V. Kuvshinnikov, N. Ya. Minina, and E. P. Skipefrov, *Cryogenics* **14**, 464 (1974).